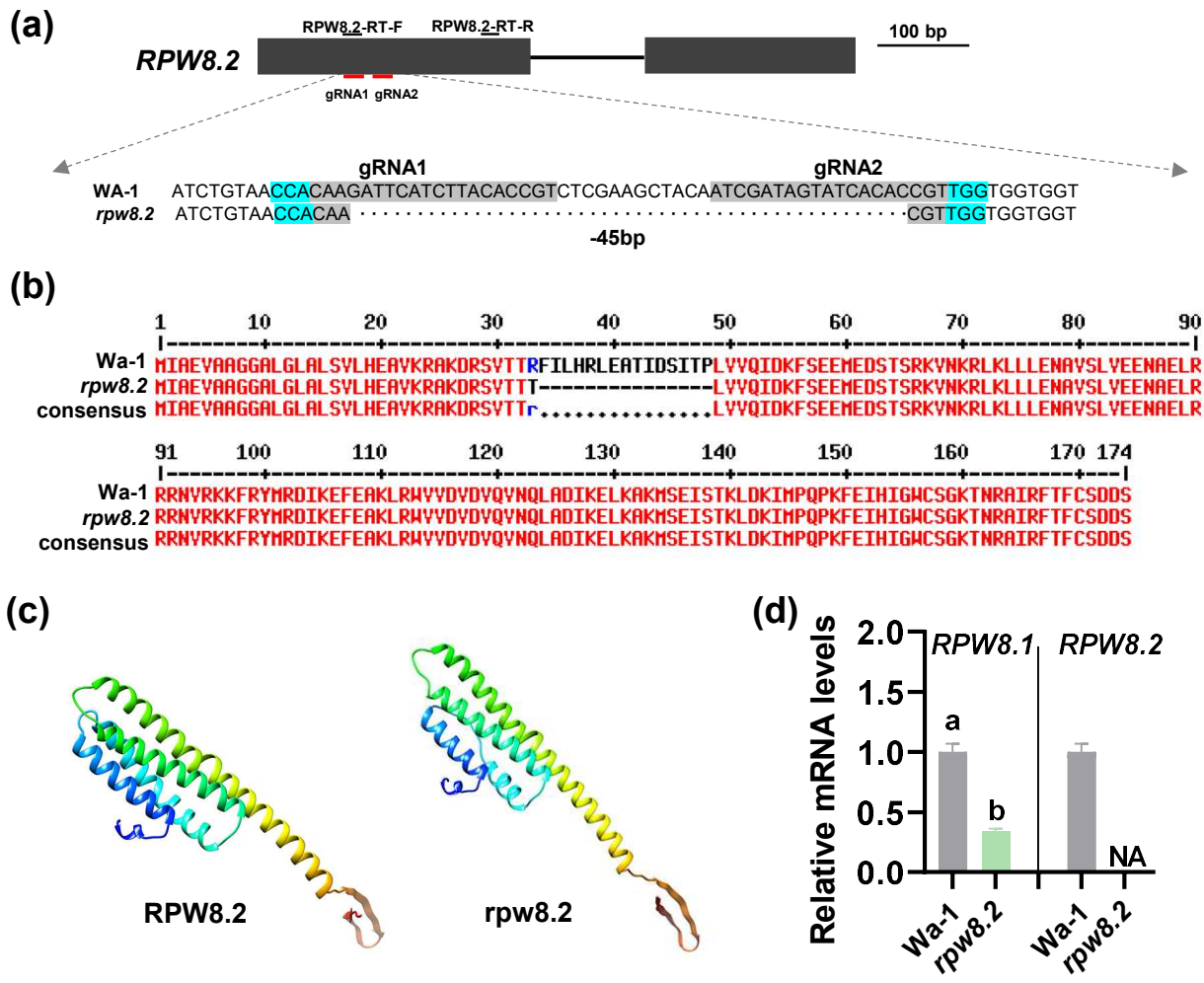

Figure S1. Mutation of *RPW8.2* leads to decreased expression of *RPW8.1*. (a) Alignment of genomic DNA sequences of *rpw8.2* and Wa-1 (WT) at the mutated site. *rpw8.2* carries a 45-base deletion. (b) Alignment of protein sequences of mutated rpw8.2 and wild type RPW8.2. rpw8.1 protein contains a 15-amino-acid deletion and an Arginine (R) to threonine (T) substitution. (c) 3D structures of mutated *rpw8.2* protein and wild type RPW8.2 protein predicted by SWISS-MODEL. (d) Reverse-transcription quantitative polymerase chain reaction (RT-qPCR) show the relative mRNA levels of *RPW8.1* and *RPW8.2* in *rpw8.2* and Wa-1 control. Data are shown as mean ± SD (n = 3 independent samples). The letters above bars indicate significant differences at $P < 0.01$ determined by one-way ANOVA followed by *post hoc* Tukey HSD analysis. "NA" means not available.

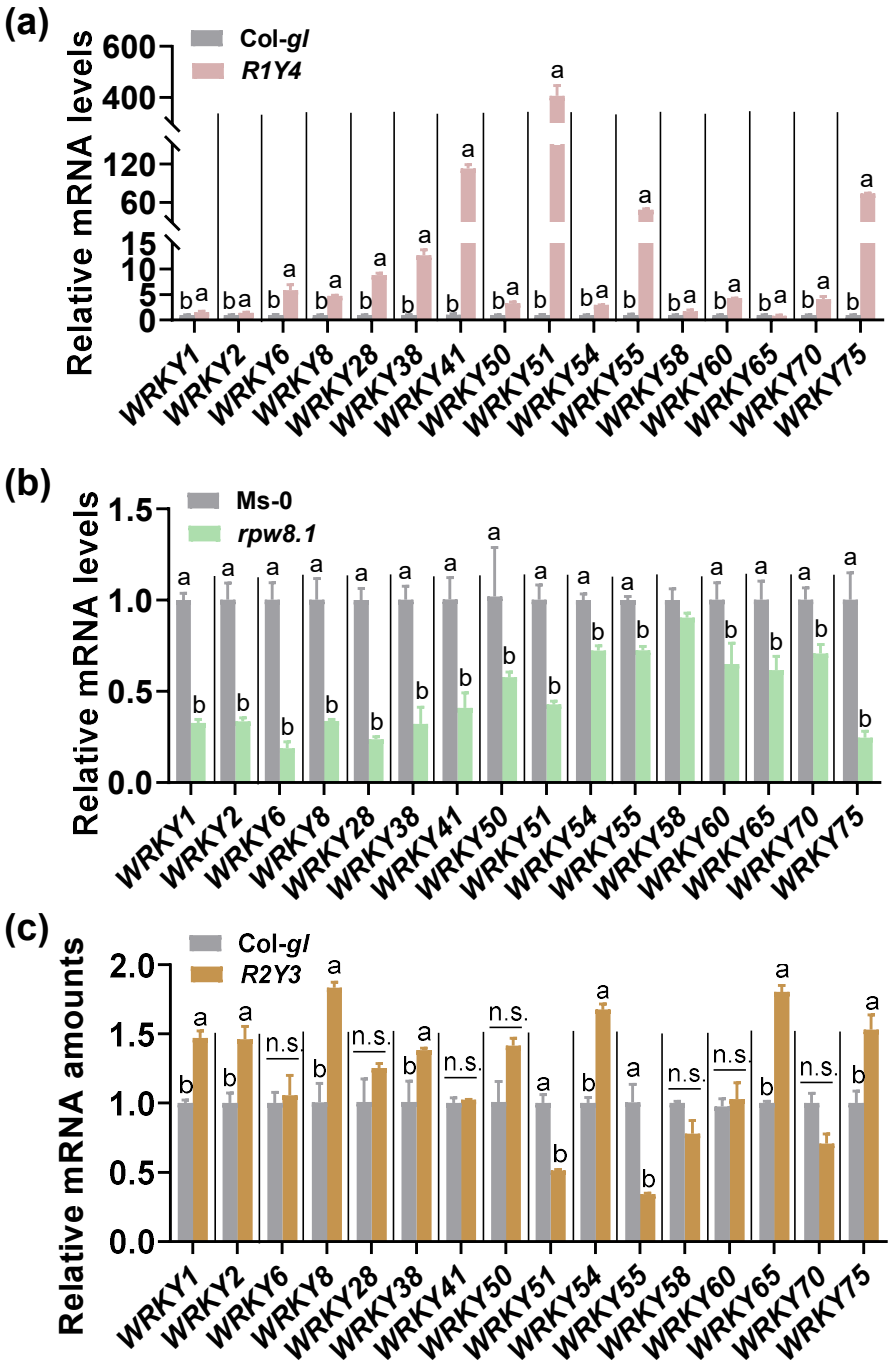

Figure S2. *RPW8.1* constitutively boosts the expression of *WRKYs*. (a-c) Reverse-transcription quantitative polymerase chain reaction (RT-qPCR) show the relative mRNA levels of *WRKYs* in *RPW8.1* transgenic line *R1Y4* and Col-*gl* control (a), or in *rpw8.1* mutant line and Ms-0 control (b), or in *RPW8.2* transgenic line *R2Y3* and Col-*gl* control. Data are shown as mean ± SD (n = 3 independent samples). The letters above bars indicate significant differences at $P < 0.01$ determined by one-way ANOVA followed by *post hoc* Tukey HSD analysis. "n.s." indicate no significant differences.

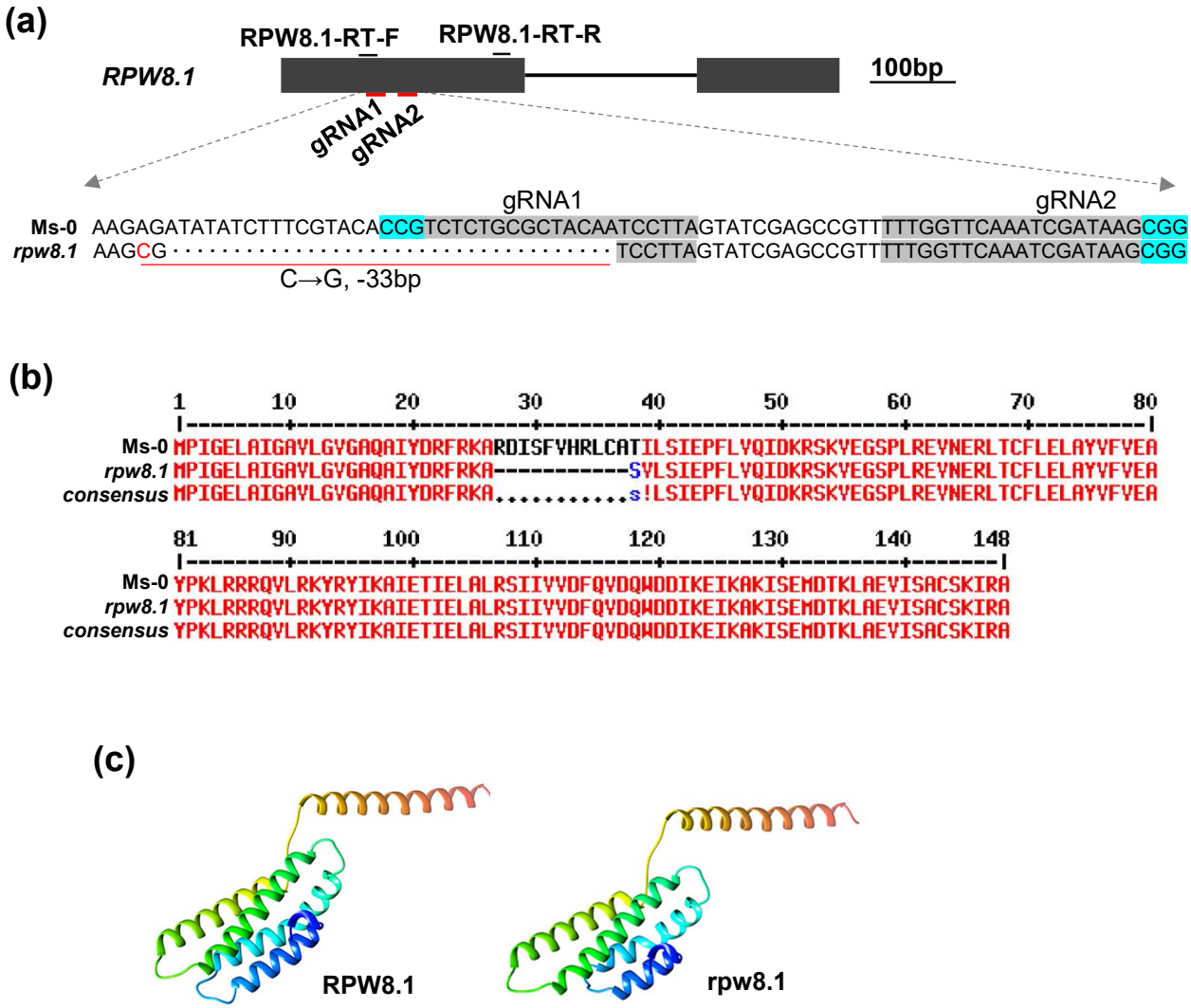

Figure S3. *rpw8.1* mutant in Ms-0 background. (a) Alignment of genomic DNA sequences of *rpw8.1* and Ms-0 (WT) at the mutated site. *rpw8.1* carries an A to C substitution and a 33-base deletion. (b) Alignment of protein sequences of mutated rpw8.1 and wild type RPW8.1. rpw8.1 contains an 11-amino-acid deletion and a threonine (T) to serine (S) substitution. (c) 3D structures of mutated rpw8.1 protein and wild type RPW8.1 protein predicted by SWISS-MODEL.

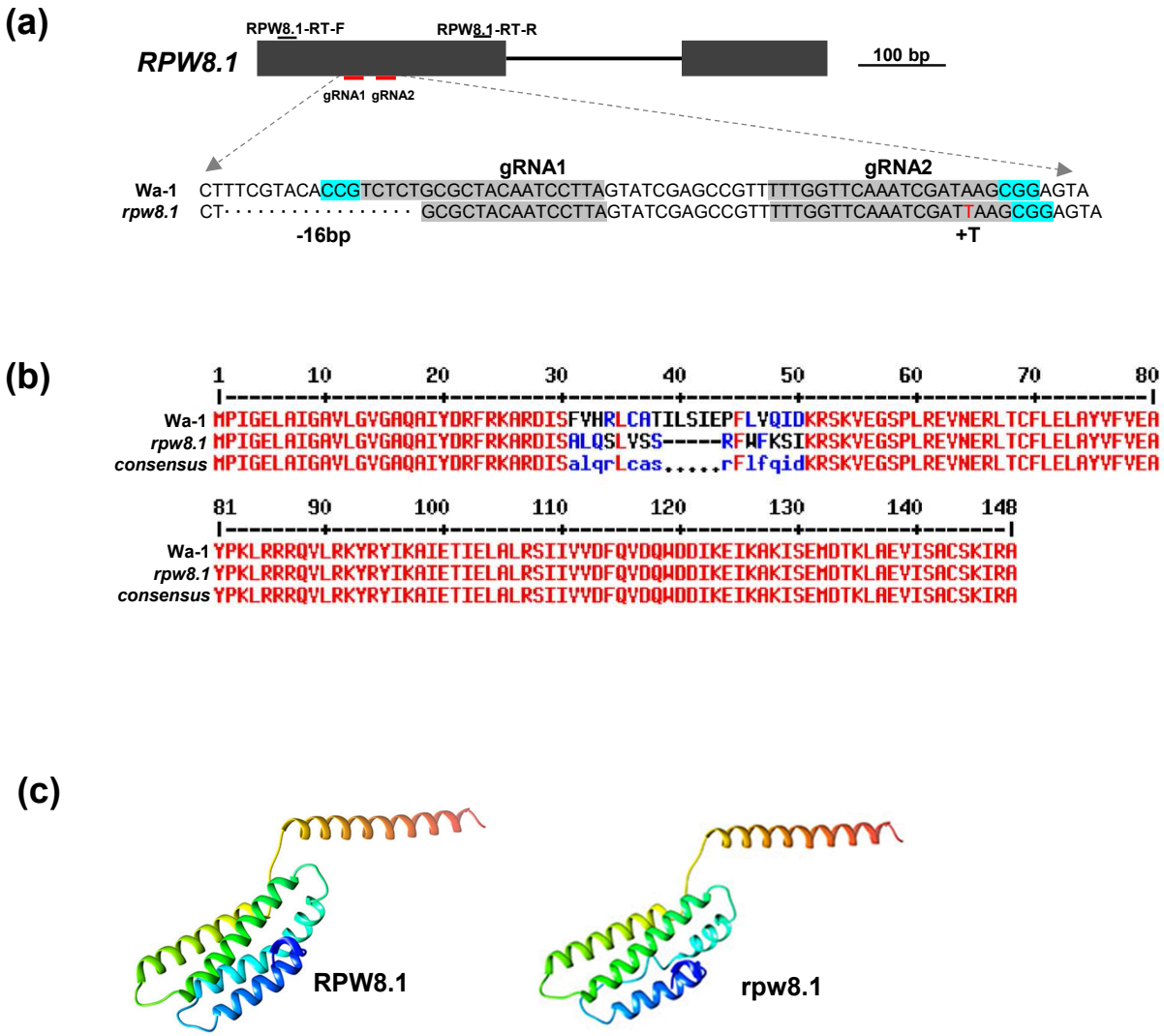

Figure S4. *rpw8.1* mutant in Wa-1 background. (a) Alignment of genomic DNA sequences of *rpw8.1* and Wa-1 (WT) at the mutated site. *rpw8.1* carries a T insertion and a 16-base deletion. (b) Alignment of protein sequences of mutated rpw8.1 and wild type RPW8.1. rpw8.1 containing a 7-amino-acid deletion and 13-amino-acid substitution. (c) 3D structures of mutated rpw8.1 protein and wild type RPW8.1 protein predicted by SWISS-MODEL.

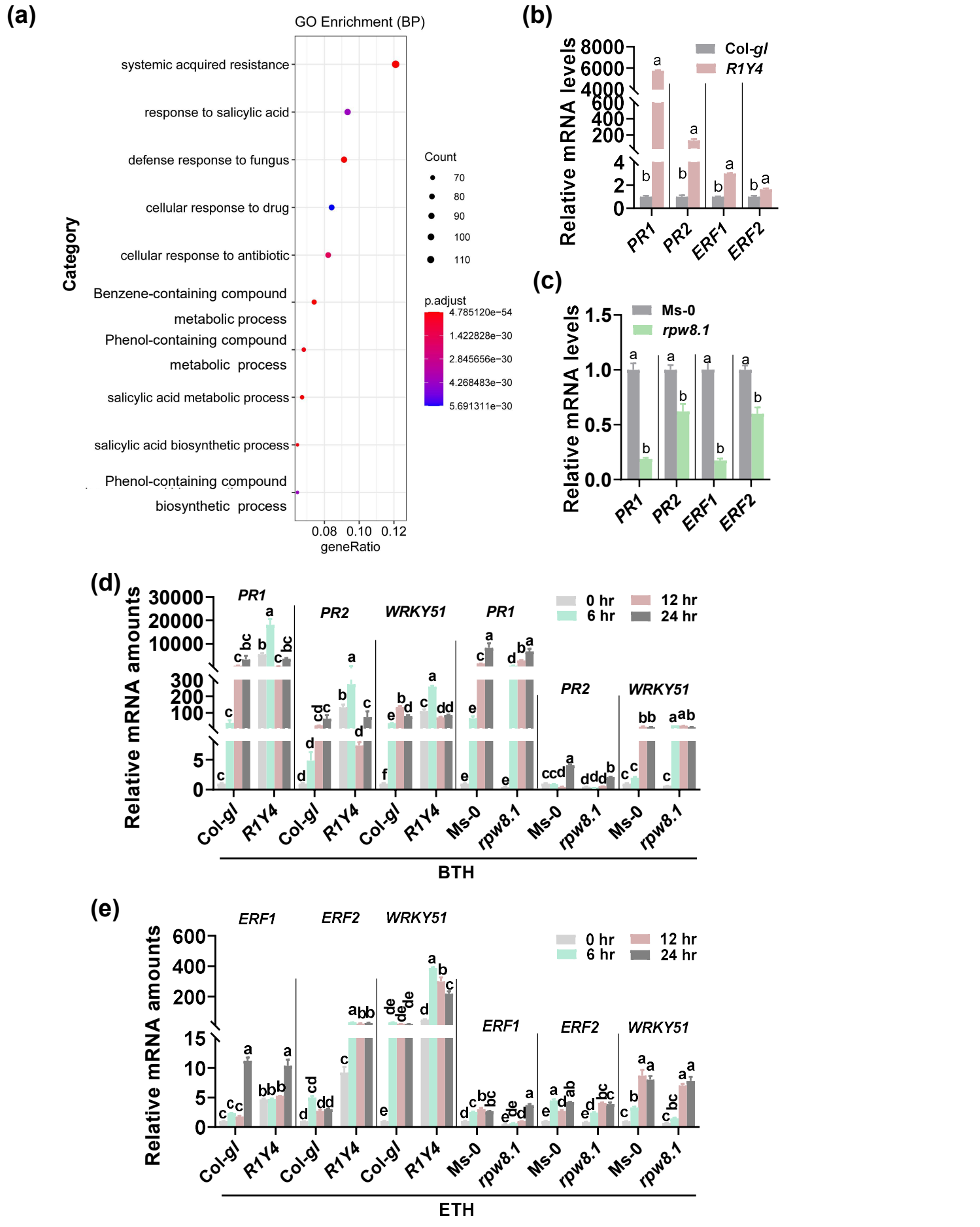
(a)
GO Enrichment (BP)
systemic acquired resistance
response to salicylic acid
defense response to fungus
cellular response to drug
cellular response to antibiotic
Benzene-containing compound metabolic process
Phenol-containing compound metabolic process
salicylic acid metabolic process
salicylic acid biosynthetic process
Phenol-containing compound biosynthetic process
Category
0.08 0.10 0.12
geneRatio
Count
70
80
90
100
110
p.adjust
4.785120e-54
1.422828e-30
2.845656e-30
4.268483e-30
5.691311e-30
(b)
Relative mRNA levels
Col-gl
R1Y4
PR1
PR2
ERF1
ERF2
(c)
Relative mRNA levels
Ms-0
rpw8.1
PR1
PR2
ERF1
ERF2
(d)
Relative mRNA amounts
PR1
PR2
WRKY51
PR1
PR2
WRKY51
0 hr
6 hr
12 hr
24 hr
Col-gl
R1Y4
Col-gl
R1Y4
Col-gl
R1Y4
Ms-0
rpw8.1
Ms-0
rpw8.1
Ms-0
rpw8.1
BTH
(e)
Relative mRNA amounts
ERF1
ERF2
WRKY51
ERF1
ERF2
WRKY51
0 hr
6 hr
12 hr
24 hr
Col-gl
R1Y4
Col-gl
R1Y4
Col-gl
R1Y4
Ms-0
rpw8.1
Ms-0
rpw8.1
Ms-0
rpw8.1
ETH

Figure S5. *RPW8.1* activates SA and ethylene signaling pathways, which enhances the expression of *WRKY51*. (a) Gene ontology (GO) enrichment analysis shows the bubble diagram of the significantly enriched pathway in *R1Y4* compared to the Col-*gl* control. The up-regulated genes (|log2FoldChange| >1; padj <0.05) in *R1Y4* (Table S3) were used for these analyses. (b-c) Reverse-transcription quantitative polymerase chain reaction (RT-qPCR) show the relative mRNA levels of the marker genes of SA and ethylene signaling pathway (*PR1* and *PR2* for SA, *ERF1* and *ERF2* for ethylene) in the transgenic lines expressing *RPW8.1* in Col-*gl* background (*R1Y4*) and the Col-*gl* control (b), or in the *rpw8.1* mutant and the Ms-0 control (c). (d-e) The relative mRNA levels of the SA and ethylene signaling pathway marker genes and *WRKY51* induced by Benzothiadiazole (BTH) (d) and Ethrel (ETH) (e) in *R1Y4*, Col-*gl*, Ms-0, and *rpw8.1* mutant, respectively. Data are shown as mean ± SD (n = 3 independent samples). The letters above bars indicate significant differences at $P < 0.01$ determined by one-way ANOVA followed by *post hoc* Tukey HSD analysis.

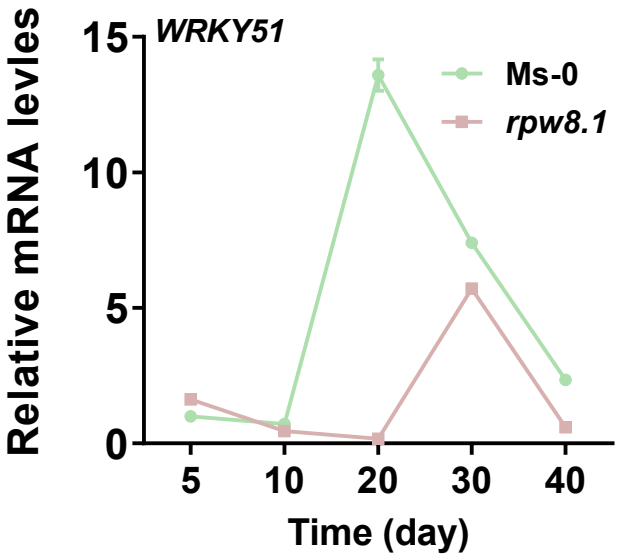

Figure S6. *WRKY51* was suppressed in *rpw8.1* mutant. Reverse-transcription quantitative polymerase chain reaction (RT-qPCR) show the relative mRNA levels of *WRKY51* in *rpw8.1* mutant and the Ms-0 control during the growth period. Data are shown as mean ± SD, n = 3 independent samples.

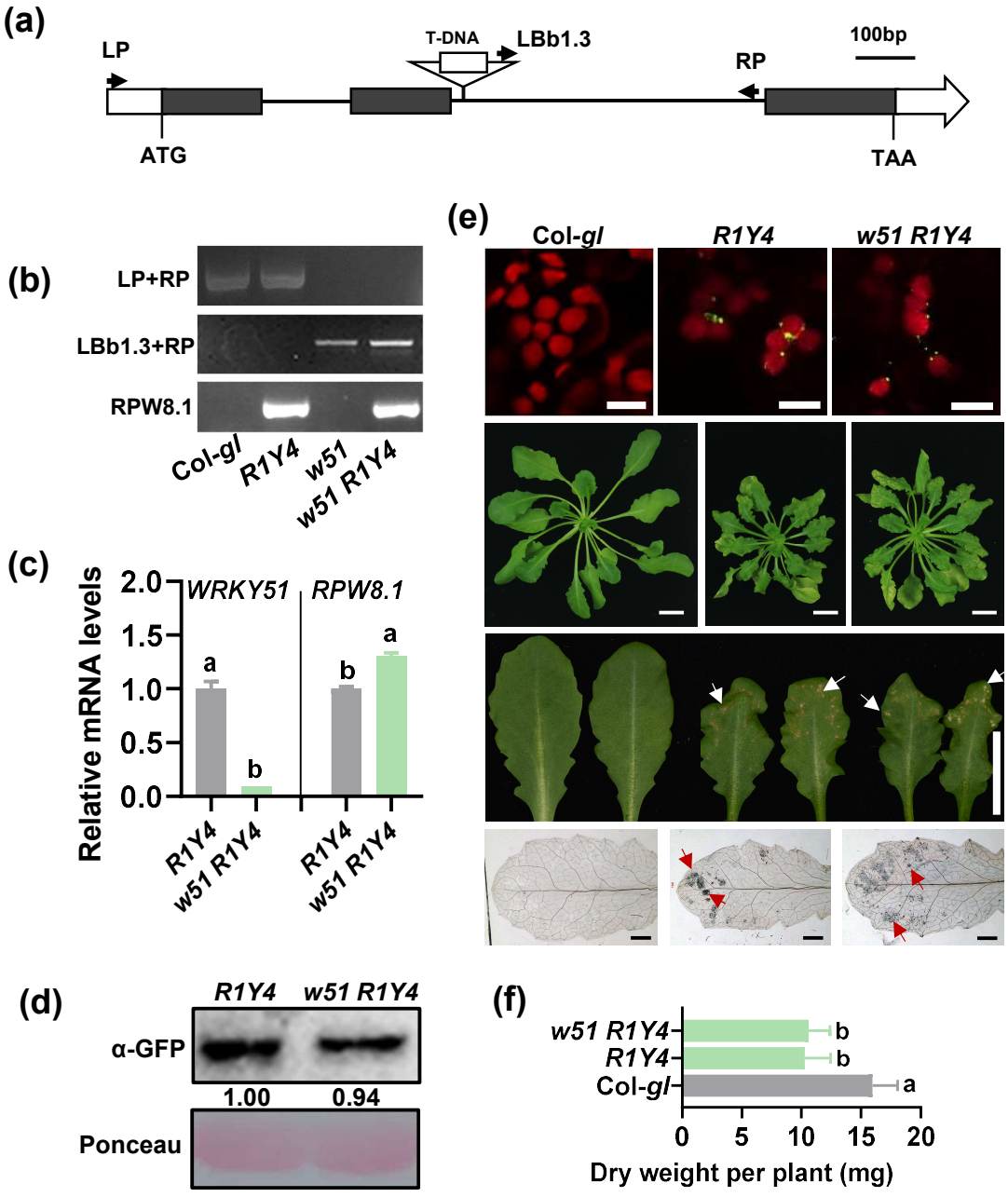

Figure S7. *WRKY51* knockout has no major effects on *RPW8.1*-mediated growth inhibition. (a) Diagram showing the position of T-DNA insertion site in the *wrky51* (*w51*) SALK mutant (SALK_022198C). White boxes represent UTR; black boxes represent exons; black lines represent introns. (b) Polymerase chain reaction (PCR) genotyping of *WRKY51* in T-DNA insertion lines *w51*, *w51 R1Y4*, Col-*gl*, and *R1Y4* controls. LP, 5′-UTR region primer; RP, intron region primer; LBb1.3, T-DNA left border primer. (c) Reverse-transcription quantitative PCR (RT-qPCR) show the relative mRNA levels of *WRKY51* and *RPW8.1* in *w51 R1Y4* and *R1Y4*. (d) RPW8.1-YFP protein amounts in *w51 R1Y4* and *R1Y4* detected in Western blots. Protein was extracted from five-week-old plants for immunoblot analysis using GFP antibodies. Values represent the relative abundance of RPW8.1 normalized to the loading. (e) Subcellular localization of Yellow fluorescent protein (YFP)-tagged RPW8.1 (RPW8.1-YFP) and Representative five-week-old plants and leaves of *w51 R1Y4* and *R1Y4*. Confocal images are acquired from leaves of five-week-old plants. RPW8.1-YFP protein was pseudo-colored green, and autofluorescent chloroplasts were pseudo-colored red. White arrows indicate the necrotic lesions and red arrows indicate cell death nearby the necrotic lesions. Cell death in the lower panel is stained by trypan blue. Scale bar = 10 μm for the upper panel and = 1 cm for middle and lower panels. (f) Dry weights of *R1Y4*, *w51 R1Y4*, and Col-*gl* plants. For (c) and (f), data are shown as mean ± SD (n = 3 independent samples). The letters above bars indicate significant differences at $P < 0.01$ determined by one-way ANOVA followed by *post hoc* Tukey HSD analysis.

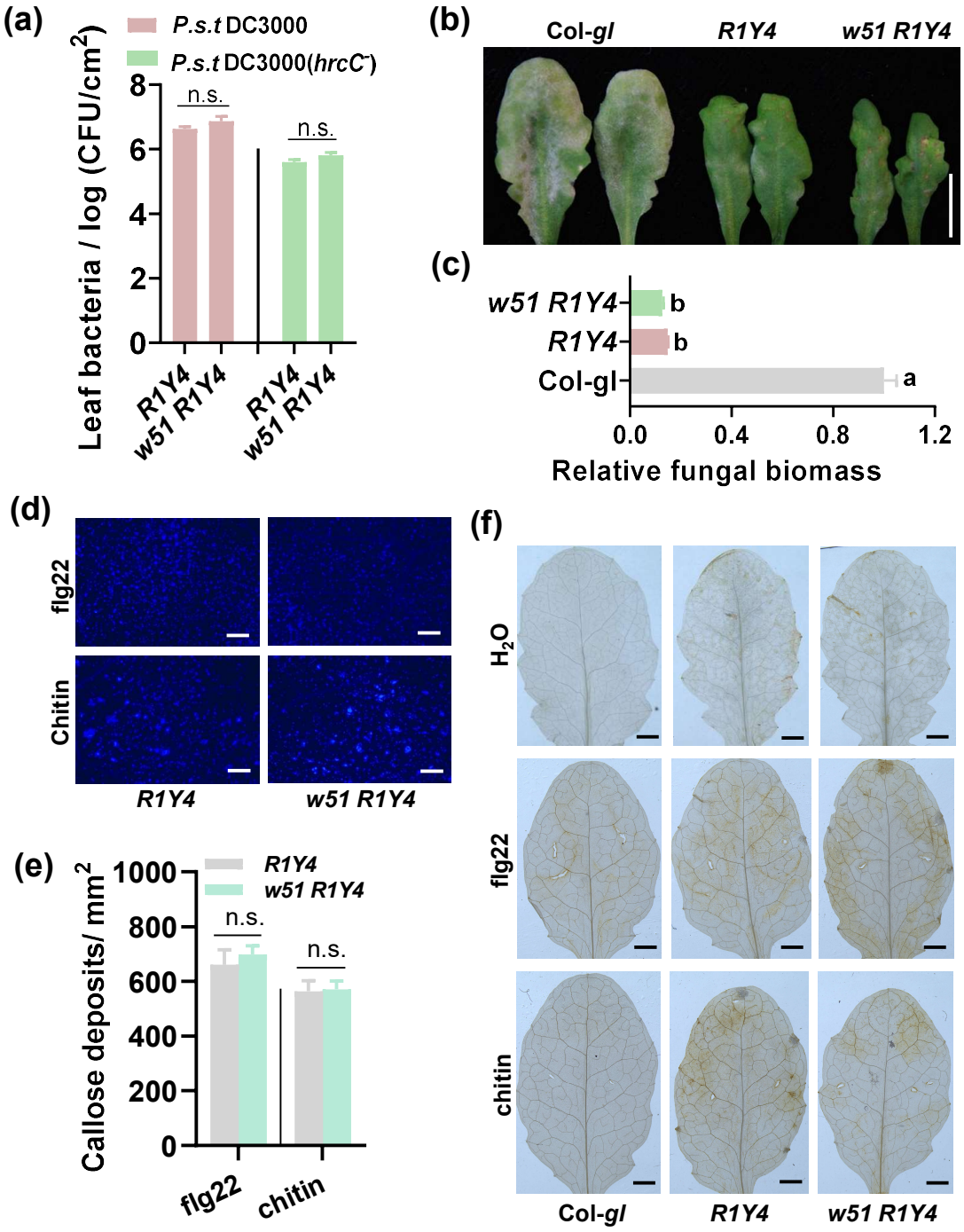

Figure S8. *WRKY51* knockout has no major effects on *RPW8.1*-mediated disease resistance and PTI responses. (a) Bacterial growth in *w51 R1Y4* and *R1Y4* three days post-inoculation (dpi) with *Pseudomonas syringae tomato* DC3000 or mutant DC3000(*hrcC*$^-$). (b) Disease symptoms of *w51 R1Y4*, *R1Y4*, and Col-*gl* control seven dpi with powdery mildew. Scale bars = 1 cm. (c) Fungal biomass of powdery mildew in (b). Fungal biomass was examined by quantitative polymerase chain reaction (qPCR) and shown as the ratio of powdery mildew *GDSL-like lipase* DNA against Arabidopsis *actin2* DNA. (d) Callose depositions in *w51 R1Y4* and *R1Y4* control 12 hours post flg22 or chitin treatment. Callose depositions were stained by aniline blue and appear as bright spots. Scale bars = 0.1 mm. (e) Quantitation of callose depositions in (d). (f) DAB-stained leaves of *w51 R1Y4*, *R1Y4*, and Col-gl control 48 hours post-treatment with or without chitin or flg22. For (a), (c) and (e), data are shown as mean ± SD (n = 6 independent samples for (a) and (e), n =3 independent samples for (c)).The letters above bars indicate significant differences at $P < 0.01$ determined by one-way ANOVA followed by *post hoc* Tukey HSD analysis. "n.s." indicate no significant differences.